Published in final edited form as:

J Phys Chem C Nanomater Interfaces. 2016 January 21; 120(2): 1004–1012. doi:10.1021/acs.jpcc.5b09777.

In Situ Generated Platinum Catalyst for Methanol Oxidation via Electrochemical Oxidation of Bis(trifluoromethylsulfonyl)imide Anion in Ionic Liquids at Anaerobic Condition

Yongan Tang, **Zhe Wang**, **Xiaowei Chi**, **Michael D. Sevilla**, and **Xiangqun Zeng***

Department of Chemistry, Oakland University, Rochester, Michigan 48309, United States

Abstract

The bis(trifluoromethylsulfonyl)imide anion is widely used as an ionic liquid anion due to its electrochemical stability and wide electrochemical potential window at aerobic conditions. Here we report an innovative strategy by directly oxidizing bis(trifluoromethylsulfonyl)imide anion to form a radical electrocatalyst on platinum electrode at anaerobic condition. The *in situ* generated radical catalyst was shown to catalytically and selectively promote the electrooxidation of methanol to form methoxyl radical, in which the formation potential was drastically decreased with the existence of bis(trifluoromethylsulfonyl)imide radical. The electrochemically generated radical catalyst not only facilitates the oxidation of methanol but also provides good selectivity. The unique double layer structure of the 1-butyl-1-methylpyrrolidinium bis(trifluoromethylsulfonyl)imide ([Bmpy][NTf_2]) likely excludes the diffusion of larger molar mass molecules onto the electrode surface and enables the highly selective methanol oxidation at this IL–electrode interface. Cyclic voltammetry (CV) experiments were used to systematically characterize the details of the electrochemical processes with and without methanol in several other ILs, and a mechanism of the chemical and redox processes was proposed. This study provides a promising new approach for utilizing the unique properties of ionic liquids not only as solvents and electrolytes but also as the medium for *in situ* generation of electrocatalysts to promote methanol redox reactions for practical applications.

Graphical Abstract

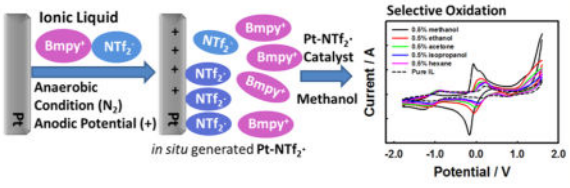

*Corresponding Author: zeng@oakland.edu, Ph 248-370-2881 (X.Z.).

Notes

The authors declare no competing financial interest.

Supporting Information

The Supporting Information is available free of charge on the ACS Publications website at DOI: 10.1021/acs.jpcc.5b09777.

Additional CVs and ionic liquid structures (PDF)

INTRODUCTION

The increasing need for clean energy has driven the interests in developing cleaner/greener methods for both energy production and chemical synthesis. Owing to its ease to control the electrochemical energy conversion, the study of the electrochemical properties of electrode and advanced materials has received significant research interest especially those related to fuel cell applications.[1] Methanol is an important chemical and also the raw material for synthetic hydrocarbon products. Fuel cells using methanol as the energy source have undergone significant development.[2,3] The mechanism of methanol oxidation in water using Pt electrocatalyst has been extensively investigated.[4] For example, it was reported that methanol oxidation in aqueous electrolyte produces CO_2 by a transfer of six electrons and six protons.[5,6]

$$CH_3OH + H_2O \rightarrow CO_2 + 6H^+ + 6e^- \quad (1)$$

Equation 1 is also the ideal anode reaction in direct methanol fuel cells (DMFCs). DMFCs are promising candidates for use as a power source due to their high energy density, relatively low operating temperatures, and zero emission of pollutants.[7–10] However, issues such as insufficient durability of the Pt-based catalysts and slow methanol electrooxidation kinetics remain a challenge for the wide application of DMFCs.[11,12] The platinum catalysts also undergo poisoning by the CO-like intermediates that were produced by the oxidation of methanol.[13] To overcome these problems, new electrochemical systems which can increase the kinetics of methanol oxidation are of significant fundamental and applied interests.

There are typically two ways to generate electrocatalysts: one is by structural or chemical modifications of the electrode surface, and another is by the interface reactions in the electrolyte.[14,15] Our early work and others show that ILs can facilitate a unique electrode–electrolyte interface formation.[16,17] We hypothesize that new catalytic reactions can be generated *in situ* at the IL–electrode interface utilizing both above pathways for oxidizing common fuels such as methanol. Nonaqueous organic IL electrolytes can promote radical catalysts for electron transfer reactions since ILs can stabilize radical cations and anions by electrostatic and van der Waals forces.[18] ILs are also excellent solvents that have high solubility for small organic molecules (i.e., methanol, ethanol, formaldehyde, formic acid, etc.) which are the energy materials for fuel cells.[19,20] Our early work shows that at platinum electrode in bis(trifluoromethylsulfonyl)imide (NTf_2) based ILs facile methane electro-oxidation was observed at room temperature in the presence of air, suggesting a unique catalytically active Pt–NTf_2 interface for electron transfer reaction of methane.[21] It is suggested that NTf_2^- can adsorb on the platinum metallic oxide surface[22] and coordinate with platinum to form an organic complex[23] which served as an catalyst for methane oxidation.[24,25] Additionally, ILs could provide a strong polar environment, wherein the C–H and C–C bond can be activated electrostatically which is also beneficial to promote methane oxidation.[26–28] Here, we explored a new approach to *in situ* electrochemically generate a Pt–NTf_2· surface catalyst and thoroughly characterized its use for catalytic oxidation of methanol at anaerobic condition. The NTf_2 anion is widely used in organic chemistry.

Lancaster et al. investigated the importance of the cation choice among different NTf_2 based ILs and discovered that different cations will affect the selectivity, yield, and reaction time of electrophilic aromatic nitration, and the NTf_2^- anions are critical for high yield nitration of toluene by acyl nitrates.[29] On the cation side of the selection, it is shown that imidazolium-based cations have a poor cathodic stability limit and phosphonium cations typically have high viscosity; thus, pyrrolidinium cation 1-butyl-1-methyl-pyrrolidinium ($Bmpy^+$) was selected. Such ILs have shown promising ionic conductivity and electrochemical stability.[30]

In this work, we systematically characterized the redox reactions of constituent anions (i.e., NTf_2^-) in [Bmpy][NTf_2] with and without the presence of methanol and compared the electrochemical behaviors in other control ILs. Our study shows that the *in situ* generated radical catalysts at the Pt surface can mediate the selective oxidation of the methanol, similar to the proton source in water solvent conditions. We intend to illustrate an exciting example that ILs not only are solvents and electrolytes but they can serve as active medium for controlled electro-chemistry to generate electrocatalysts *in situ* for promoting important redox chemistries such as methanol oxidation that is described in this report.

EXPERIMENTAL SECTION

Chemicals and Reagents

1-Butyl-1-methylpyrrolidinium bis(trifluoromethylsulfonyl)imide ([Bmpy][NTf_2], 99%), 1-butyl-3-methylimidazolium bis(trifluoromethylsulfonyl)imide ([Bmim][NTf_2], 99%), and 1-butyl-3-methylimidazolium tetra-fluoroborate ([Bmim][BF_4], 99%) were purchased from IOLITEC Inc. Methanol (99.9%), ethanol (99.9%), acetone (99.9%), and isopropanol (99.9%) were purchased from Sigma-Aldrich without further purification.

Measurements

Platinum working electrode (diameter = 2 mm) was purchased from CH Instrument Inc. and polished to a mirror-like plane with 0.5 and 0.05 μm alumina slurries, followed by extensive washing with DI water and ethanol, and then dried under nitrogen gas. A conventional electrochemical cell was purposefully designed to facilitate the proper positioning of three electrodes. The surface of the working electrode was drop coated before measurement with 200 μL of the IL. Two platinum wires with a diameter of 0.5 mm were used as the counter and quasi-reference electrodes. The distance between reference and working was maintained in constant distance of 2 mm to minimize the effects of electrolyte resistance. Specific concentrations of analyte were introduced on top of the IL with nitrogen as the carrier gas. All potentials used in this work were versus platinum. Infrared spectra were recorded on a Varian FTS 7000 FT-IR spectrometer. Electrochemical quartz crystal micro-balance (EQCM) experiments were performed with an electrochemical potentiostat for electrochemical control interfaced with a Maxtek research quartz crystal microbalance (RQCM) instrument for the frequency measurements. A 10 MHz Pt QCM electrode (International Crystal Manufacturing Company, Inc.) was used as the working electrode.

All electrochemical measurements were performed on a Gamry potentiostat running Windows XP (Gamery Instrument). The total gas flow was maintained at 200 sccm

(standard cubic centimeters per minute) by digital mass-flow controllers (MKS Instruments, Inc.). Two gas paths were used to adjust the volume ratio of the testing gas flows, in which one was used to control the background gas (N_2) flow and the other was used to control the analyte gas flow to reach specific concentration calculated by corresponding saturated vapor pressure. Volume percent concentration (v/v)% was used for the concentration of analytes in this work.

RESULTS AND DISCUSSION

In Situ Generated Pt Catalysts by Redox Reactions of NTf_2^- Anion

ILs composed of organic cation or anion are typically more electrochemically stable than other nonaqueous electrolytes providing a much wider potential window. The bis(trifluoromethanesulfonyl)imide (NTf_2^-) anion is widely used as an IL forming anion which has a notable electrochemical stability.[25] It has been reported that 1-ethyl-3-methyl-imidazolium bis(trifluoromethanesulfonyl)imide can tolerate an anodic potential of 6 V vs RHE on a tungsten substrate.[29] However, the anion can be oxidized at a high anodic potential, and the cation can be reduced at a high cathodic potential as well. Rather than minimize the redox activities of the electrolytes and/ or solvents as in most electrochemical system, the electrochemical activities of the IL electrolytes were explored here to generate radical precursors to form active species at the electrode interface to promote and control the desirable reactions. As shown in Figure 1a, ionic liquid [Bmpy][NTf_2] can be electrochemically oxidized at Pt electrode in an inert nitrogen environment at small potential window by multiple CV cycles. The CV cycles in Figure 1a were obtained by first setting potential at 0 V vs Pt quasi-reference electrode and scanned to −1.4 V, and then the potential was cycling between −1.4 and 1.4 V to obtain multiple CV plots. Since oxygen cannot be removed completely from the electrochemical system, a small oxygen reduction and superoxide oxidation peak pair I/I′ at −1.0 V was observed due to the presence of trace amount oxygen.[31] Previous studies have shown that oxygen can be reduced in these ILs at the potential of (−1.0 to −1.2 V) at platinum surface,[32,33] similar to those shown in Figure 1a. The reduction of Pt–O could lead to the accumulation of oxygen on the electrode surface and cause a small increase of oxygen radical formation current in I/I′ peaks at subsequent potential cycles.

The oxidation of NTf_2^- anion can lead to the formation of $NTf_2\cdot$ radical.[34] Here, peak III is the oxidation of NTf_2^- anion for forming $NTf_2\cdot$ radical, which shows partial reversibility with a much smaller reduction current of peak III′. The $NTf_2\cdot$ radical formed is likely adsorbed on the Pt electrode and results in the appearance of peak II/II′ at 0.1 V. Interestingly, the peak pair II/ II′ gradually increased with each CV cycle and reached a constant value after 30 cycles (as shown in the charge plot in Figure 1b peak II/II′). The appearance of peak II should be directly related to peak III, in which the NTf_2^- anions were oxidized to form $NTf_2\cdot$ radicals. Figure S1 (Supporting Information) shows different potential windows of the CV data obtained in [Bmpy][NTf_2], which confirmed that the appearance of peak II required the anodic electrode potential to be at or larger than that of peak III potential (Figure S1b,c). Figure S1d further proved that the appearance of peak II did not have direct relation to peak I because no significant difference was observed for the

current response of peak II compared to Figure S1c when potential limits were in the range of (−0.6 to 1.6 V).

Figure 1b shows the integrated charges (*Q*) of peak II/II′ and peak III/III′ obtained from different CV cycles in Figure 1a. It was found that the oxidation charge (peak III in Figure 1b) of NTf_2^- anions was equal to the reduction charge (peak II′ + III′) of $NTf_2\cdot$ and Pt–$NTf_2\cdot$ radicals except for the first few CV cycles. The loss of reduction charge in the initial cycles should indicate a surface adsorption process before the establishment of an equilibrium for Pt–$NTf_2\cdot$ radicals. Figure S2 presents the peak currents vs scan rates result for the redox process of Pt–$NTf_2\cdot$ radicals. A linear relationship between peak currents of peak II/ II′ and scan rates was obtained, which confirmed that the Pt–$NTf_2\cdot$ radical redox reaction was a surface process arising from the Pt–$NTf_2\cdot$ surface layer on Pt electrode.

The cycle numbers are not the only factor that affects the amount of $NTf_2\cdot$ radicals formed. The final anodic potentials are shown to affect the amount of $NTf_2\cdot$ radical produced during the CV scanning. Different potential windows of CVs have been used to characterize how much $NTf_2\cdot$ radical can be produced at different anodic potentials. Figure S3a shows the CV curves at the 50th cycle with different potential windows. Figure S3b compared the total charge of peak II obtained for each experiment at different anodic potentials. The appearance of peak II/II′ required an anodic potential more positive than 1.4 V, which means 1.4 V is the potential where NTf_2^- anions start to be oxidized and form $NTf_2\cdot$ radicals. It is reasonable that more positive anodic potentials will provide higher energy for oxidizing NTf_2^- anions to $NTf_2\cdot$ radicals and lead to a higher amount of $NTf_2\cdot$ radicals formed.

As an efficient coordinating anion, when NTf_2^- is oxidized to $NTf_2\cdot$ radical, the Pt–$NTf_2\cdot$ coordinate complex is likely formed in the absence of other ligands on Pt.[35,36] The reduction of Pt–$NTf_2\cdot$ will cause the desorption of some NTf_2^- anions during the cathodic scan. As shown in the multiple cycle CV experiments (Figure 1a), the peak current of peak II/II′ kept increasing until a dynamic equilibrium was established. In addition, the surface process is selective and only occurs at Pt electrode. No such electrochemical phenomena were observed at Au electrode (Figure S4). Thus, platinum is critical in the reaction mechanism proposed. FT-IR was used to verify the adsorption of $NTf_2\cdot$ radical on platinum electrode, as shown in Figure S5. However, no obvious peaks related to the formation of Pt–$NTf_2\cdot$ were observed during 50 CV cycles. It is likely that the amount of $NTf_2\cdot$ radical formed is small which is beyond the FT-IR sensitivity to measure. However, additional data analysis for peak II/II′ vs scan rates for the first three cycles shows that the peak current is linear with scan rate in all these cycles confirming the processes is a surface-controlled process (Figure S2). In addition, the EQCM experiment also confirmed that formation of Pt–NTf_2 in peak II/II′ region (details see Figure S6). Thus, we rationalized the processes related to peak II to the reactions between the Pt surface and $NTf_2\cdot$ detailed in eqs 2–4.

$$\mathrm{NTf_2^- - e^- \leftrightarrow Ntf_2\cdot} \quad (\mathrm{peak\ III}) \qquad (2)$$

$$NTf_2\cdot + Pt \leftrightarrow Pt{-}NTf_2\cdot \quad (3)$$

$$Pt{-}NTf_2\cdot + e^- \leftrightarrow Pt{-}NTf_2{}^- \quad (\text{peak II/II}') \quad (4)$$

Since the catalyst is generated *in situ*, it is more important to validate the results that are reproducible than their long-term stability. We have tested more CV cycles to validate the reproducibility of the generation of Pt–NTf_2 catalyst in IL, as shown in Figure S7. The peak current of II/II′ remained stable after 1000 CV cycles which further proved the high reproducibility of the *in situ* generated catalyst in this system. There was a small potential drift which was due to the duration experiment (overnight) which generated products which changed the local electrochemical interface affecting the quasi-reference electrode potential.

Ionic Liquid Effects

We performed further studies to understand if only $NTf_2{}^-$ anions can form surface layer with Pt electrode. Two other ILs ([Bmim][NTf_2] and [Bmim][BF_4]) with different anion or cation were selected and characterized at identical experimental conditions. Table S1 lists the cation and anion structure of these two different ILs. In [Bmim][NTf_2], the Pt-NTf_2· radical peaks also appeared in the multiple CV experiments similar to those shown in Figure 2a peak II/II′ in [Bmpy][NTf_2]. The cathodic peak at −1.0 V is due to trace oxygen reduction. The second cathodic peak at −0.8 V in Figure 2a should be attributed to the adsorption of $Bmim^+$ cation, which also can be observed in [Bmim][BF_4] ILs (Figure 2b). The small anodic peak at −0.1 V in [Bmim][BF_4] (Figure 2b) is due to oxidation of the $BF_4{}^-$ anion. $BF_4{}^-$ is not as stable and much easier to be oxidized than $NTf_2{}^-$ anion.[37] There is no redox process observed at 0.1 V in [Bmim][BF_4], which further supports the proposed mechanism that the $NTf_2{}^-$ anion is being oxidized to form Pt–NTf_2· radicals during the anodic potential scanning in [Bmpy][NTf_2]. The anodic and cathodic peak current ratio of peak II/II′ vs cycle numbers in [Bmim][NTf_2] and [Bmpy]-[NTf_2] was calculated in order to investigate the influence of different cations for the redox process of Pt–NTf_2· radicals, as shown in Figure 2c. It was found that different cations will affect the reversibility of the Pt–NTf_2· radical redox process. The I_{pa}/ I_{pc} of peak II/II′ in [Bmim][NTf_2] deviated much more from one than [Bmpy][NTf_2] during the first 20 CV cycles, which was the initial stage of generating Pt–NTf_2· radicals. This confirmed that the $Bmim^+$ will compete with NTf_2· radicals for forming a surface adsorption layer on the Pt electrode.

All the above experiments were performed under anaerobic conditions, although trace amount of oxygen was present in the CV experiments, as shown in the Figure 1a peak I/I′. No Pt–NTf_2· radicals redox process (Figure 1a peak II/II′) was observed in the ambient condition (Figure S8), signifying the importance of the anaerobic conditions for the above processes to occur. Higher concentrations of oxygen can facilitate the oxidation of the Pt surface to form Pt–O which could hinder the oxidation of $NTf_2{}^-$ and obstruct the formation of Pt–NTf_2· radicals.[38] In contrast, $NTf_2{}^-$ anions are well-known for their high

electrochemical stability in atmosphere condition;[14] the anaerobic environment provided an extreme condition that decreased their electrochemical stability.

Methanol Oxidation by the *in Situ* Generated Pt–NTf_2·Catalysts

Methanol oxidation has been investigated extensively due to its potential application in fuel cells.[4,39,40] The oxidation of methanol on the platinum surface typically involves the adsorption of CH_3OH with successive dehydrogenation as shown in eqs 5 and 6.

$$\mathrm{CH_3OH} \leftrightarrow \mathrm{CH_3OH_{(ad)}} \quad (5)$$

$$\mathrm{CH_3OH_{(ad)}} \leftrightarrow \mathrm{CH_{\mathit{x}-1}OH_{(ad)}} + \mathrm{OH_{(ad)}} \quad (\mathit{x}=3,2,1) \quad (6)$$

In aqueous solution, the oxidation of methanol requires a second oxygen atom, which comes from the splitting H_2O (OH intermediate) on the platinum surface. The issues of aqueous solvent are the high activation potential for forming OH intermediate and the strong adsorption of CO that decreases the catalytic performance of platinum.[41,42] To overcome the poison effect of CO on platinum, one approach is to alloy secondary metals into platinum and form alloy catalysts.[43] Another approach is to use solvents other than water that can alter the oxidation process of methanol.[44]

The *in situ* generated Pt–NTf_2· radicals were expected to promote the oxidation of methanol since they have high activity as a catalyst for C–H bond activation.[26] Figure 3a is the multiple CV cycles (−1.4 to 1.4 V) when 0.64% (v/v) of methanol was introduced into [Bmpy][NTf_2] at Pt electrode in a nitrogen environment. The presence of methanol not only shows oxidation current at potential higher than 1.0 V, it also shows a large redox peak current at 0 V. The electrochemical behavior in Figure 3a is similar to that of pure [Bmpy][NTf_2] (Figure 1a). However, detailed charge analysis of redox peaks in Figure 3b suggested different electrochemical behaviors in the presence of methanol. The peak charge of II/II′ kept increasing throughout the 50 CV cycles, and the potential shifted from 0.1 V in [Bmpy][NTf_2] IL without methanol to 0 V in the presence of methanol. The anodic current (I_{pa}) vs cathodic current (I_{pc}) of peak II/II′ is much closer to one, which indicated a high reversibility of the redox process of peak II/II′ (Figure 3c). Besides the increase of the peak pair II/II′ at 0 V, there is a new peak appeared at 1.1 V, which should be attributed to the oxidation of methanol. Peak II and peak III currents increase with each CV cycle, suggesting that the active sites of the platinum surface were not blocked by strong adsorption species like CO, and the oxidation of methanol was promoted by the reaction intermediates in the IL.

Figure S9 shows the control experiment of methanol oxidation in [Bmim][BF_4] IL. The experimental condition in Figure S9 was strictly following the condition of that in Figure 3a, allowing the comparison of methanol oxidation in these two ILs. The results show that without the presence of NTf_2^- anion the same concentration of methanol (0.64% v/v) did

not show any methanol oxidation response in [Bmim][BF_4]. These results have further confirmed the significant role of NTf_2^- anion in catalyzing the oxidation of methanol.

Proposed Methanol Oxidation Mechanisms

Radicals are commonly formed during the redox process in ionic liquids.[45,46] For oxidation of methanol, there are two ways for losing hydrogen to form radicals: losing the hydrogen attached to oxygen forming $\cdot OCH_3$ and losing the hydrogen attached to carbon forming $\cdot CH_2OH$. The formation of hydroxymethyl radical $\cdot CH_2OH$ (ΔH, 98.0 kcal/mol) is more thermodynamically favored than the formation of the methoxyl radical $\cdot OCH_3$ (ΔH, 104.1 kcal/mol).[47] Furthermore, hydroxymethyl $\cdot CH_2OH$ radicals have an unsaturated carbon and a greater tendency to bond to the surface. It is also consistent with density-functional theory (DFT) calculation results, in which the coordination via carbon is more favorable than that via oxygen.[48] Here methanol was the only analyte present in the [Bmpy][NTf_2]; thus, the oxidation peak at 1.1 V in Figure 4a should come from the oxidation of methanol for forming hydroxymethyl $\cdot CH_2OH$ radicals, and the larger oxidation peak after 1.1 V is due to methoxyl $\cdot OCH_3$ radicals. The increased peak II/II′ should be directly related to the radical transfer between Pt–$NTf_2\cdot$ radicals and methanol. The sum of methanol oxidation charge (peak III and peak III′) is equal to the reduction charge obtained from peak II′ (Figure 3b), which shows a relation between the direct oxidation of methanol and the redox process of Pt–$NTf_2\cdot$ radicals. A mechanism of methanol oxidation in the [Bmpy]-[NTf_2] is proposed as follows.

$$NTf_2^- + CH_3OH - e^- \leftrightarrow \cdot CH_2OH + HNTf_2 \quad (7)$$

$$NTf_2^- + CH_3OH - e^- \leftrightarrow \cdot OCH_3 + HNTf_2 \quad (8)$$

$$Pt - NTf_2 \cdot + CH_3OH_{(ad)} \leftrightarrow HPtNTf_2 + \cdot CH_2OH_{(ad)} \quad (9)$$

$$Pt - NTf_2 \cdot + CH_3OH_{(ad)} \leftrightarrow HPtNTf_2 + \cdot OCH_{3(ad)} \quad (10)$$

$$HPtNTf_2 + \cdot CH_2OH_{(ad)} + e^- \leftrightarrow Pt - NTf_2^- + CH_3OH_{(ad)} \quad (11)$$

$$HPtNTf_2 + \cdot OCH_{3(ad)} + e^- \leftrightarrow Pt - NTf_2^- + CH_3OH_{(ad)} \quad (12)$$

Equation 7 should be accounted for the direct oxidation of methanol at 1.1 V to form hydroxymethyl $\cdot CH_2OH$ since $\cdot CH_2OH$ radical is thermodynamically more favorable, and eq 8 should be directly related to the methoxyl radical $\cdot OCH_3$ due to its reported existence as the majority radical formation during methanol oxidation.[49] The much higher peak current 1.4 V compared to 1.1 V also confirms the main pathway of eq 8 between $\cdot CH_2OH$ and $\cdot OCH_3$ radicals (eqs 7 and 8) formation. Equations 9 and 10 can be used to explain the current increase and potential shift of peak II/II′ with the presence of methanol. The formation of Pt–$NTf_2\cdot$ radicals interacted with methanol and formed ($\cdot CH_2OH/\cdot OCH_3$) radicals, which in turn increased the redox reaction of Pt–$NTf_2\cdot$ radicals (eq 4). The increasing peak current of peak II/II′ indicated the high reactivity of Pt–$NTf_2\cdot$ radicals and their fast interaction with methanol.

The oxidation potential of methanol was investigated by setting different scan potential windows for the CV, as shown in Figure 4. Figure 4a shows the different anodic and cathodic potential ranges of CV curve in [Bmpy][NTf_2] with 0.5% (v/v) methanol present. Similar electrochemical behaviors were observed as in pure [Bmpy][NTf_2] (Figure S3). However, in pure IL, the current in peak II kept increasing with higher positive potential since the NTf_2^- anion was the solvent and electrolyte, which can provide sufficient supply during the oxidation potential. In the presence of methanol, an increase in potential produces more methanol radicals which cause the increase in peak II/II′ due to the shifts of equilibria described in eqs. eqs 9 and 10 that produce more Pt–$NTf_2^{\bullet}$ radicals. However, the increase of peak current of peak II/II′ will eventually reach equilibrium since the concentration of methanol is constant, as shown in Figure 4b. When the potential is higher than 1.8 V, the radicals ($\cdot CH_2OH/\cdot OCH_3$) produced by methanol oxidation reach a maximum that lead to a stable level of Pt–$NTf_2\cdot$ radicals in peak II at Figure 4a. These results confirm that the production of methanol radicals is directly related to the anodic oxidation potential and the concentration of methanol.

Since $\cdot OCH_3$ is the major radical formed during methanol oxidation, the reaction in eq 12 involves $\cdot OCH_3$ radicals should be the main pathway between eqs 11 and 12. A scan rate experiment was performed in the presence of methanol, as shown in Figure S10. The peak current of peak II/II′ is proportional to the square root of the scan rate, which means the redox processes of eq 12 are a diffusion-controlled process in the presence of methanol radicals. This is different from the results in pure [Bmpy][NTf_2] IL (Figure S2b), which confirmed the proposed mechanism in eq 12 that methanol radicals were involved in the redox process of Pt–$NTf_2\cdot$ and did not form strong bonding at Pt electrode such as CO which poisons the Pt catalyst. The methanol radicals involved in the redox process of Pt–$NTf_2\cdot$ radicals process not only increased the current of peak II/II′ but also increased its reversibility since the I_{pa}/I_{pc} of peak II/II′ is much closer to one in the presence of methanol (Figure 3c). The Pt-$NTf_2\cdot$ radicals here acted as catalysts to facilitate the oxidation of methanol by reducing the oxidation potential of 1.4 V (eq 8) to 0.1 V (eq 10) to form $\cdot OCH_3$ radicals.

The above-mentioned reaction paths for methanol oxidation provide a new mechanism that could have direct application to the oxidation of other molecules. It is well-known that CO intermediates poison the Pt catalyst which leads to dramatically decrease of catalytic

activity. However, the oxidation of methanol in our IL system did not show the formation of CO intermediates that is detrimental to the Pt electrode catalyst. The Pt–NTf_2· radicals not only serve as intermediates that promote oxidation of methanol for forming methanol radicals; it also provided a highly reversible redox reaction which can be used for methanol concentration measurement. Figure 5a shows background subtracted CV of different concentrations of methanol in the [Bmpy][NTf_2] system at an anaerobic environment. As mentioned before, the 1.1 V is the peak of hydroxymethyl · CH_2OH radical formation and this peak can be used for quantitative determination of the methanol concentration, as shown in the calibration curve in Figure 5b. The relationship between the current and methanol concentration at 1.1 V was found to have an excellent linear fit with the calibration equation shown in Figure 5b. The good linear fit and calibration for methanol detection are evidence for the intermediates during the electrochemical processes based on the mechanism proposed.

The sensitivity is 9.03 μA/% when peak current at 1.1V was used for calibration curve. However, if peak II is used for quantification, the sensitivity of methanol detection increases to 21.1 μA/%, which is the same as the sensitivity by using peak at potential of 1.4 V (the formation of ·OCH_3 radicals in eq 10) for plotting the calibration curve (Figure 5b). The fact that the sensitivity obtained from peak at 1.4 V is the same as the sensitivity by using peak II (eq 4) indicates the oxidation of methanol for forming methoxyl ·OCH_3 radicals (eq 8) is the main reaction between two pathways (formation of ·CH_2OH and ·OCH_3 radicals in eqs 7 and 8). Therefore, the redox reactions in peak II/II′ should be contributed from eq 12 (·OCH_3 radical formation) since the sensitivity here is directly related the concentration of ·OCH_3 radicals, which is the product of eq 8. The same sensitivity for 1.4 V oxidation and peak II (Figure 5b) further confirms the relationship of radical transferring mechanism (eq 10) between Pt–NTf_2· and methanol.

Selectivity of the Methanol Oxidation by the *in Situ* Generated Pt–NTf_2· Catalysts

Four commonly used organic molecules (ethanol, acetone, hexane, isopropanol) were tested to study the selectivity of the *in situ* generated Pt–NTf_2· catalyst for methanol oxidation. 0.5% (v/v) of chosen molecule was added into [Bmpy][NTf_2], and CV scanning was performed, as shown in Figure 6a. The acetone, isopropanol, and hexane showed only small potential shifts and current increase in peak II, which means these molecules did not readily react with the Pt–NTf_2· radical catalyst at least at the rates that were comparable to methanol. However, ethanol did show a somewhat larger current response in peak II. This is reasonable since the ethanol has similar molecular structure as methanol and can be oxidized as well in [Bmpy][NTf_2], but the much lower peak current also indicates the lower diffusion of ethanol into Pt surface in the IL due to its larger molecular size. This interpretation is supported by a recent study that molecular dynamics simulations of ten different pure and CO_2 saturated ionic liquids have shown a strong correlation between the ratio of unoccupied space in pure ILs and their ability to absorb CO_2.[50]

Figure 6b plots the current response at peak II when the same concentration of analyte was present; the higher Pt–NTf_2· radical oxidation currents obtained from methanol and ethanol are consistent with the radical reaction mechanism. The fact that isopropanol/ethanol which

has the lowest H-bond energy of the alcohols did not readily react is clear evidence that molecular size and shape are important features in the catalytic process. The unique double layer structure of [Bmpy][NTf_2] provides the selectivity for small molecule such as methanol.[16] Both of the cation and anion of [Bmpy][NTf_2] are large with weak electrostatic cation–anion interaction densities which allow a large number of unoccupied space in the IL for methanol adsorption but not for larger molecules.[50]

CONCLUSION

In this work, we have demonstrated a new approach exploring the reactivity of NTf_2^- based ILs for *in situ* generating reactive radicals that can form a platinum adsorbate that catalyzes the oxidation of methanol in an anaerobic condition. NTf_2^- anion was found to be unique in generating radical catalysts at the platinum electrode. The *in situ* generated $NTf_2\cdot$ radicals can be easily controlled by the numbers of potential cycles and the anodic electrode potential. The Pt–$NTf_2\cdot$ radicals were found to catalyze the oxidation of methanol and the current response of Pt–$NTf_2\cdot$ radical was proportional to the concentration of methanol which can be used as the calibration for methanol detection. In contrast to traditional Pt catalyst, CO poisoning for methanol oxidation was not present since methanol was only partially oxidized and formed radicals. We also demonstrated the high selectivity of $NTf_2\cdot$ radicals for methanol oxidation, since low interference from ethanol, acetone, hexane, and isopropanol is observed which was explained by the size selection of the unique [Bmpy][NTf_2]–electrode interface structure. This study provides a promising new approach of utilizing the unique properties of NTf_2-based ILs not only as solvents and electrolytes but also as active mediums to *in situ* generate electrocatalysts to enable new methanol oxidation pathways. The rate and selectivity of a chemical reaction can be controlled by electrochemical polarization of the electronic conductive catalyst (Pt) in an ionic liquid electrolyte (i.e., an ionic conductive medium) by cycle numbers and potentials as well as the choice of the electrode materials and IL electrolytes. The solubility of methanol in many ILs is also higher than many other solvents. These features can be exploited to increase the amount of methanol adsorption and the rate of methanol oxidation at the same time. The high selectivity toward methanol oxidation is very beneficial for the methanol sensor developments. The new mechanism in which radicals can promote the oxidation of methanol and avoid the formation of carbon monoxide should also have applications in methanol-based fuel cell applications. Furthermore, the ILs' tremendous diversity in structural and chemical properties will provide the opportunities for other unique IL–electrode interfaces to be designed for electrochemical catalytic conversion of other hydrocarbons for fuel cell and sensor applications.

Supplementary Material

Refer to Web version on PubMed Central for supplementary material.

Acknowledgments

X. Zeng thanks the following grants which support the ionic liquid electrochemistry research for the sensor development (National Institute of Occupational Safety and Health (1R01OH009644-01A1) and National institute of Environmental Health (R01ES022302).

References

1. Tran Thanh T, Castro M, Kim TY, Suh KS, Feller JF. High Stability Silver Nanoparticles-Graphene/Poly(Ionic Liquid)-Based Chemoresistive Sensors for Volatile Organic Compounds' Detection. Anal Bioanal Chem. 2014; 406:3995–4004. [PubMed: 24414740]
2. Shi G, Wang Z, Xia J, Bi S, Li Y, Zhang F, Xia L, Li Y, Xia Y, Xia L. Mixed Ionic Liquids/Graphene-Supported Platinum Nanoparticles as an Electrocatalyst for Methanol Oxidation. Electrochim Acta. 2014; 142:167–172.
3. Tao Q, Chen W, Yao Y, Bin Yousaf A, Chen Y-x. Study on Methanol Oxidation at Pt and Ptru Electrodes by Combining in Situ Infrared Spectroscopy and Differential Electrochemical Mass Spectrometry. Chin J Chem Phys. 2014; 27:541–547.
4. Jusys Z, Behm RJ. Methanol Oxidation on a Carbon-Supported Pt Fuel Cell Catalyst - a Kinetic and Mechanistic Study by Differential Electrochemical Mass Spectrometry. J Phys Chem B. 2001; 105:10874–10883.
5. Bagotzky VS, Vassiliev YB, Khazova OA. Generalized Scheme of Chemisorption, Electrooxidation and Electroreduction of Simple Organic-Compounds on Platinum Group Metals. J Electroanal Chem Interfacial Electrochem. 1977; 81:229–238.
6. Leger JM, Lamy C. The Direct Oxidation of Methanol at Platinum Based Catalytic Electrodes - What Is New since 10 Years. Berichte Der Bunsen-Gesellschaft Phys Chem Chem Phys. 1990; 94:1021–1025.
7. Reddington E, Sapienza A, Gurau B, Viswanathan R, Sarangapani S, Smotkin ES, Mallouk TE. Combinatorial Electrochemistry: A Highly Parallel, Optical Screening Method for Discovery of Better Electrocatalysts. Science. 1998; 280:1735–1737. [PubMed: 9624047]
8. Arico AS, Srinivasan S, Antonucci V. Dmfcs. From Fundamental Aspects to Technology Development. Fuel Cells. 2001; 1:133–161.
9. Jafarian M, Mahjani MG, Heli H, Gobal F, Khajehsharifi H, Hamedi MH. A Study of the Electro-Catalytic Oxidation of Methanol on a Cobalt Hydroxide Modified Glassy Carbon Electrode. Electrochim Acta. 2003; 48:3423–3429.
10. Yang HZ, Tang YA, Zou SZ. Electrochemical Removal of Surfactants from Pt Nanocubes. Electrochem Commun. 2014; 38:134–137.
11. Gavrilov AN, Savinova ER, Simonov PA, Zaikovskii VI, Cherepanova SV, Tsirlina GA, Parmon VN. On the Influence of the Metal Loading on the Structure of Carbon-Supported Ptru Catalysts and Their Electrocatalytic Activities in Co and Methanol Electro-oxidation. Phys Chem Chem Phys. 2007; 9:5476–5489. [PubMed: 17925974]
12. Tang YA, Edelmann RE, Zou SZ. Length Tunable Penta-Twinned Palladium Nanorods: Seedless Synthesis and Electrooxidation of Formic Acid. Nanoscale. 2014; 6:5630–5633. [PubMed: 24752282]
13. Carrette L, Friedrich KA, Stimming U. Fuel Cells: Principles, Types, Fuels, and Applications. ChemPhysChem. 2000; 1:162–193. [PubMed: 23696319]
14. Villagran C, Aldous L, Lagunas MC, Compton RG, Hardacre C. Electrochemistry of Phenol in Bis{(Trifluoromethyl)-Sulfonyl}Amide (Ntf2 (–)) Based Ionic Liquids. J Electroanal Chem. 2006; 588:27–31.
15. Siriviriyanun A, Imae T. Advantages of Electrodes with Dendrimer-Protected Platinum Nanoparticles and Carbon Nanotubes for Electrochemical Methanol Oxidation. Phys Chem Chem Phys. 2013; 15:4921–4929. [PubMed: 23435635]
16. Wang Z, Mu X, Guo M, Huang Y, Mason AJ, Zeng X. Methane Recognition and Quantification by Differential Capacitance at the Hydrophobic Ionic Liquid-Electrified Metal Electrode Interface. J Electrochem Soc. 2013; 160:B83–B89.
17. Fedorov MV, Kornyshev AA. Ionic Liquids at Electrified Interfaces. Chem Rev. 2014; 114:2978–3036. [PubMed: 24588221]
18. Mukherjee S, List B. Organic Chemistry - Radical Catalysis. Nature. 2007; 447:152–153. [PubMed: 17495911]

19. Safavi A, Momeni S, Tohidi M. Silver-Palladium Nanoalloys Modified Carbon Ionic Liquid Electrode with Enhanced Electrocatalytic Activity Towards Formaldehyde Oxidation. Electroanalysis. 2012; 24:1981–1988.
20. Lee YG, Chou TC. Ionic Liquid Ethanol Sensor. Biosens Bioelectron. 2004; 20:33–40. [PubMed: 15142574]
21. Wang Z, Zeng X. Bis(Trifluoromethylsulfonyl)Imide (Ntf2)-Based Ionic Liquids for Facile Methane Electro-Oxidation on Pt. J Electrochem Soc. 2013; 160:H604–H611.
22. Sobota M, Nikiforidis I, Hieringer W, Paape N, Happel M, Steinruck HP, Gorling A, Wasserscheid P, Laurin M, Libuda J. Toward Ionic-Liquid-Based Model Catalysis: Growth, Orientation, Conformation, and Interaction Mechanism of the [Tf(2)N](–) Anion in [Bmim][Tf(2)N] Thin Films on a Well-Ordered Alumina Surface. Langmuir. 2010; 26:7199–7207. [PubMed: 20143797]
23. Williams DB, Stoll ME, Scott BL, Costa DA, Oldham WJ. Coordination Chemistry of the Bis(Trifluoromethylsulfonyl)Imide Anion: Molecular Interactions in Room Temperature Ionic Liquids. Chem Commun. 2005:1438–1440.
24. Duris F, Barbier-Baudry D, Dormond A, Desmurs JR, Bernard JM. Lanthanide Bis(Trifluoromethylsulfonyl)Amides Vs. Trifluoromethylsulfonates as Catalysts for Friedel-Crafts Acylations. J Mol Catal A: Chem. 2002; 188:97–104.
25. Howlett PC, Izgorodina EI, Forsyth M, MacFarlane DR. Electrochemistry at Negative Potentials in Bis-(Trifluoromethanesulfonyl)Amide Ionic Liquids. Z Phys Chem (Muenchen, Ger). 2006; 220:1483–1498.
26. Marx A, Yamamoto H. Aluminum Bis-(Trifluoromethylsulfonyl)Amides: New Highly Efficient and Remarkably Versatile Catalysts for C-C Bond Formation Reactions. Angew Chem, Int Ed. 2000; 39:178–181.
27. Steinrueck HP, Libuda J, Wasserscheid P, Cremer T, Kolbeck C, Laurin M, Maier F, Sobota M, Schulz PS, Stark M. Surface Science and Model Catalysis with Ionic Liquid-Modified Materials. Adv Mater. 2011; 23:2571–2587. [PubMed: 21520462]
28. Sobota M, Sobota M, Schmid M, Happel M, Amende M, Maier F, Steinruck HP, Paape N, Wasserscheid P, Laurin M, Gottfried JM, et al. Ionic Liquid Based Model Catalysis: Interaction of Bmim Tf2n with Pd Nanoparticles Supported on an Ordered Alumina Film. Phys Chem Chem Phys. 2010; 12:10610–10621. [PubMed: 20607171]
29. Lancaster NL, Llopis-Mestre V. Aromatic Nitrations in Ionic Liquids: The Importance of Cation Choice. Chem Commun. 2003:2812–2813.
30. Cheng JY, Chu YH. 1-Butyl-2,3-Trimethyleneimidazolium Bis(Trifluoromethylsulfonyl)Imide (B-3c-Im Ntf2): A New, Stable Ionic Liquid. Tetrahedron Lett. 2006; 47:1575–1579.
31. Wang Z, Lin P, Baker GA, Stetter J, Zeng X. Ionic Liquids as Electrolytes for the Development of a Robust Amperometric Oxygen Sensor. Anal Chem. 2011; 83:7066–7073. [PubMed: 21848335]
32. Rogers EI, Huang XJ, Dickinson EJF, Hardacre C, Compton RG. Investigating the Mechanism and Electrode Kinetics of the Oxygen Vertical Bar Superoxide (O-2 Vertical Bar O-2(Center Dot)) Couple in Various Room-Temperature Ionic Liquids at Gold and Platinum Electrodes in the Temperature Range 298–318 K. J Phys Chem C. 2009; 113:17811–17823.
33. Xiao C, Rehman A, Zeng X. Evaluation of the Dynamic Electrochemical Stability of Ionic Liquid-Metal Interfaces against Reactive Oxygen Species Using an in Situ Electrochemical Quartz Crystal Microbalance. RSC Adv. 2015; 5:31826–31836.
34. Shkrob IA, Marin TW, Zhu Y, Abraham DP. Why Bis(Fluorosulfonyl)Imide Is a “Magic Anion” for Electrochemistry. J Phys Chem C. 2014; 118:19661–19671.
35. Mathieu B, Ghosez L. Trimethylsilyl Bis-(Trifluoromethanesulfonyl)Imide as a Tolerant and Environmentally Benign Lewis Acid Catalyst of the Diels-Alder Reaction. Tetrahedron. 2002; 58:8219–8226.
36. Liston DJ, Lee YJ, Scheidt WR, Reed CA. Observations on Silver Salt Metathesis Reactions with Very Weakly Coordinating Anions. J Am Chem Soc. 1989; 111:6643–6648.
37. Sowmiah S, Srinivasadesikan V, Tseng MC, Chu YH. On the Chemical Stabilities of Ionic Liquids. Molecules. 2009; 14:3780–3813. [PubMed: 19783957]

38. Wang Z, Guo M, Baker GA, Stetter JR, Lin L, Mason AJ, Zeng X. Methane-Oxygen Electrochemical Coupling in an Ionic Liquid: A Robust Sensor for Simultaneous Quantification. Analyst. 2014; 139:5140–5147. [PubMed: 25093213]
39. Wasmus S, Kuver A. Methanol Oxidation and Direct Methanol Fuel Cells: A Selective Review. J Electroanal Chem. 1999; 461:14–31.
40. Surampudi S, Narayanan SR, Vamos E, Frank H, Halpert G, Laconti A, Kosek J, Prakash GKS, Olah GA. Advances in Direct Oxidation Methanol Fuel-Cells. J Power Sources. 1994; 47:377–385.
41. Ticanelli E, Beery JG, Paffett MT, Gottesfeld S. An Electrochemical, Ellipsometric, and Surface Science Investigation of the Ptru Bulk Alloy Surface. J Electroanal Chem Interfacial Electrochem. 1989; 258:61–77.
42. Gasteiger HA, Markovic N, Ross PN, Cairns EJ. Co Electrooxidation on Well-Characterized Pt-Ru Alloys. J Phys Chem. 1994; 98:617–625.
43. Ohkubo Y, Kageyama S, Seino S, Nakagawa T, Kugai J, Nitani H, Ueno K, Yamamoto TA. Radiolytic Synthesis of Carbon-Supported Ptru Nanoparticles Using High-Energy Electron Beam: Effect of Ph Control on the Ptru Mixing State and the Methanol Oxidation Activity. J Nanopart Res. 2013; 15:1597.
44. Guo S, Dong S, Wang E. Constructing Carbon Nanotube/Pt Nanoparticle Hybrids Using an Imidazolium-Salt-Based Ionic Liquid as a Linker. Adv Mater. 2010; 22:1269. [PubMed: 20437517]
45. Strehmel V. Radicals in Ionic Liquids. ChemPhysChem. 2012; 13:1649–1663. [PubMed: 22431313]
46. Levendorf AM, Sun SG, Tong YJ. In Situ Ft-Ir Investigation of Methanol and Co Electrooxidation on Cubic and Octahedral/ Tetrahedral Pt Nanoparticles Having Residual Pvp. Electrocatalysis. 2014; 5:248–255.
47. Malakhova IV, Shubin AA. On the Nature of Radicals Formed in Methanol Catalytic Oxidation. Kinet Catal. 2009; 50:583–586.
48. Ishikawa Y, Liao MS, Cabrera CR. Oxidation of Methanol on Platinum, Ruthenium and Mixed Pt-M Metals (M = Ru, Sn): A Theoretical Study. Surf Sci. 2000; 463:66–80.
49. Malakhova IV, Ermolaev VK, Danilova IG, Paukshtis EA, Zolotarskii IA. Kinetics of Free Radical Generation in the Catalytic Oxidation of Methanol. Kinet Catal. 2003; 44:536–546.
50. Klähn M, Seduraman A. What Determines Co2 Solubility in Ionic Liquids? A Molecular Simulation Study. J Phys Chem B. 2015; 119:10066–10078. [PubMed: 26168324]

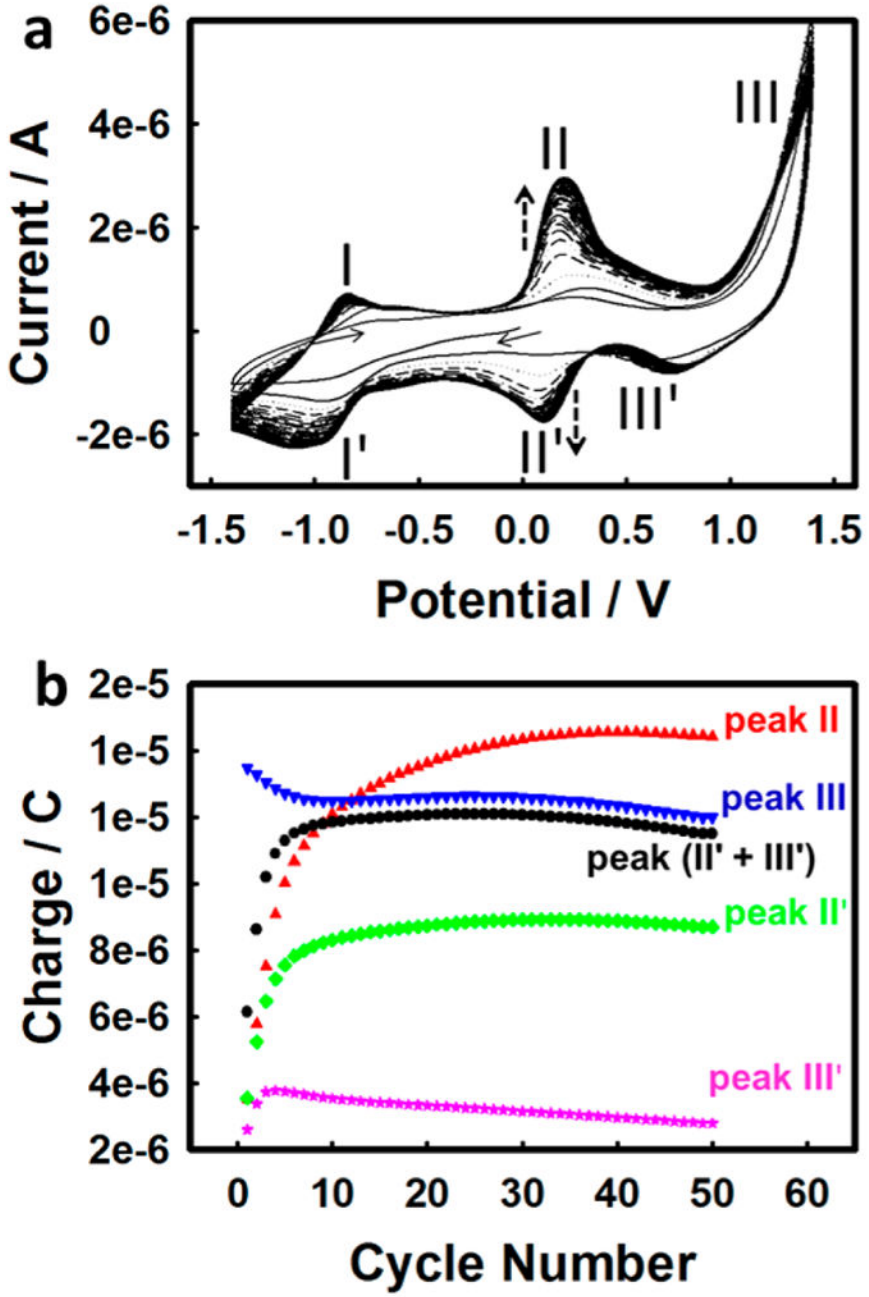

Figure 1.

(a) Multiple cyclic voltammetry in [Bmpy][NTf_2] ionic liquid, nitrogen environment at Pt electrode; scan rate: 100 mV s^{-1}. (b) Integrated charge (−0.5 to 0.85 V for peak II; −0.4 to 0.4 V for peak II′; 0.85 to 1.4 V for peak III; 0.4 to 1.0 V for peak III′) at different CV cycles obtained from (a).

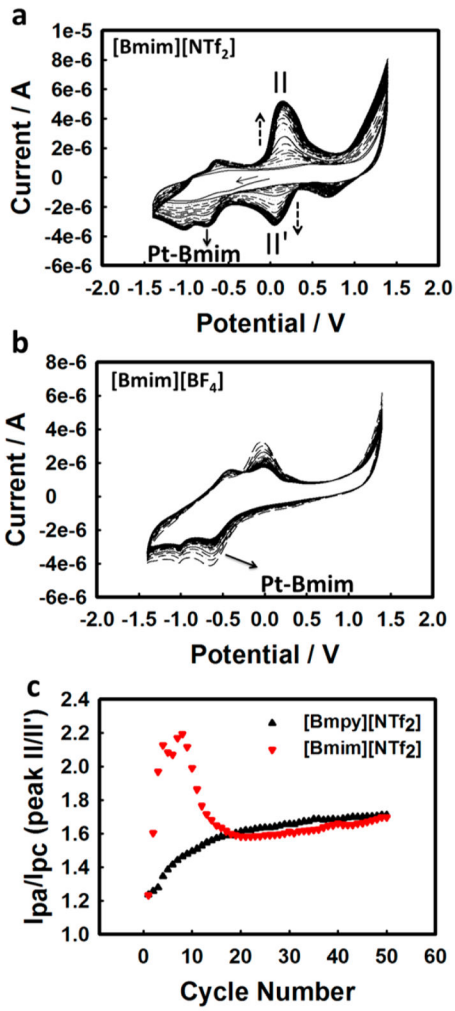

Figure 2.

Multiple CV in (a) [Bmim][NTf_2] and (b) [Bmim][BF_4] ionic liquid in nitrogen environment. Scan rate: 100 mV s^{-1}. (c) Anodic and cathodic peak current ratio (peak II/II′) in [Bmpy][NTf_2] and [Bmim][NTf_2] IL.

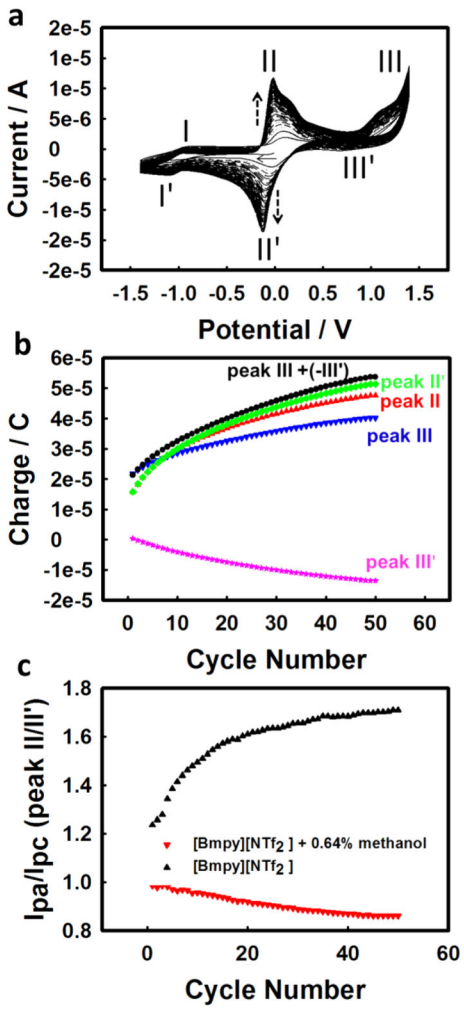

Figure 3.

(a) Multiple CV cycles of 0.64% (v/v) methanol in [Bmpy][NTf_2] ionic liquid, nitrogen environment at Pt electrode; scan rate: 100 mV s^{-1}. (b) Integrated charge (−0.5 to 0.75 V for peak II; −0.6 to 0.3 V for peak II′; 0.75 to 1.4 V for peak III; 0.3 to 1.0 V for peak III′) during different CV cycles obtained from (a). (c) Anodic current (I_{pa}) vs cathodic current (I_{pc}) of peak II/II′ in [Bmpy][NTf_2] (black) and methanol introduced (red).

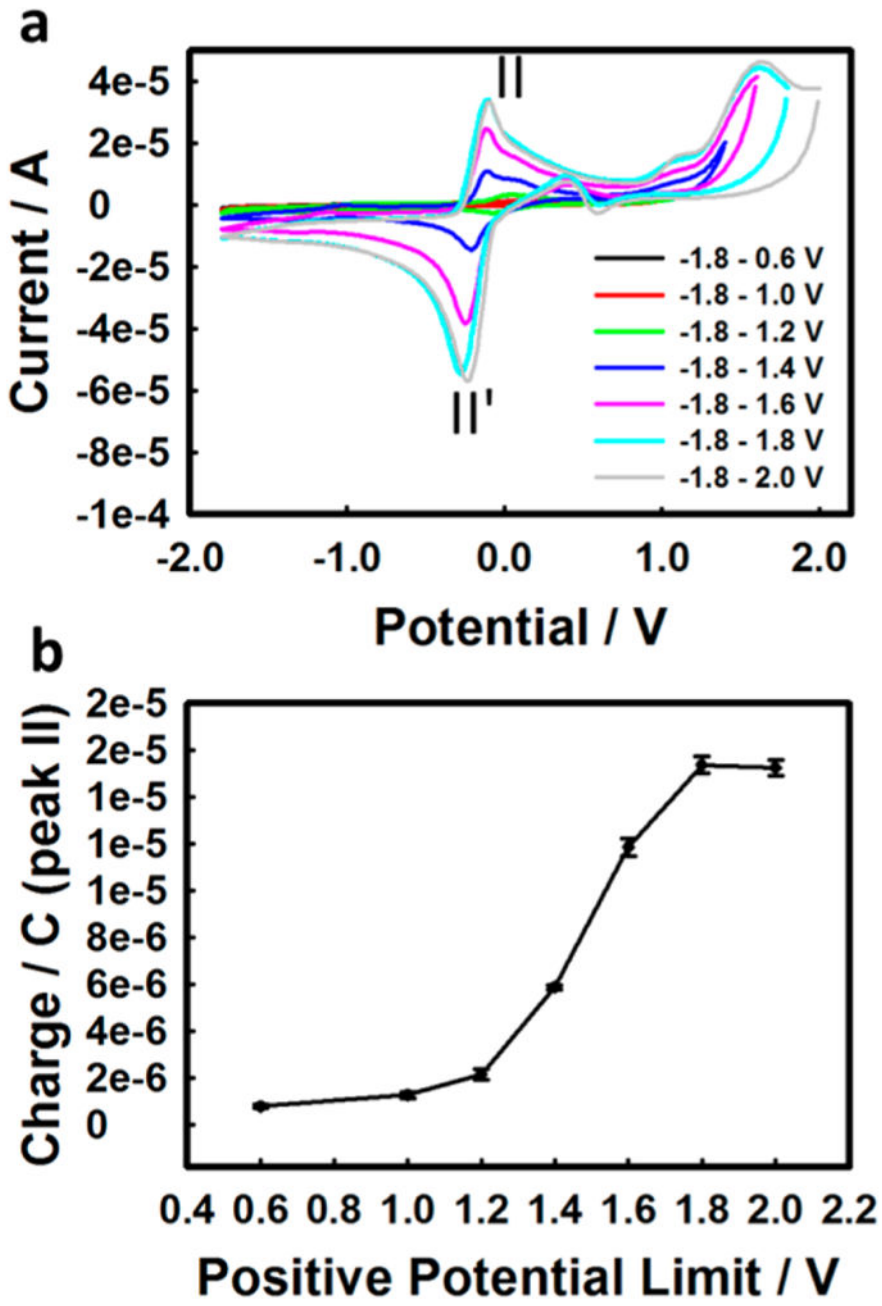

Figure 4.

(a) Different positive potential limit of CV scan for 0.5% (v/v) of methanol in [Bmpy][NTf_2] ionic liquid at Pt electrode. Scan rate: 100 mV s^{-1}. (b) Integrated charge plot obtained from current of peak II (−0.5 to 0.85 V) in (a).

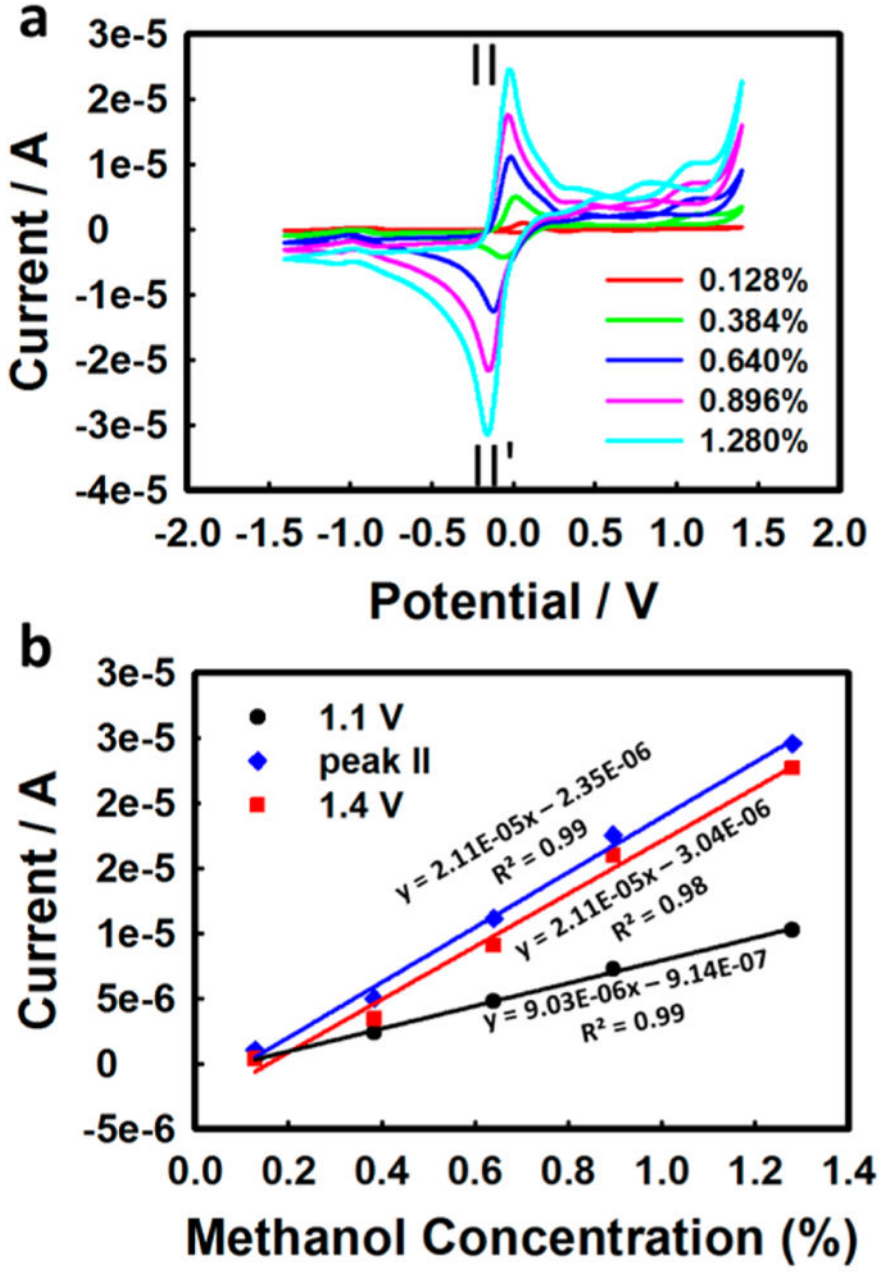

Figure 5.

(a) Background subtracted CV of different methanol concentration (v/v)% in [Bmpy][NTf_2] IL in nitrogen carrying gas. (b) Calibration curves of methanol in [Bmpy][NTf_2] IL in nitrogen at Pt electrode.

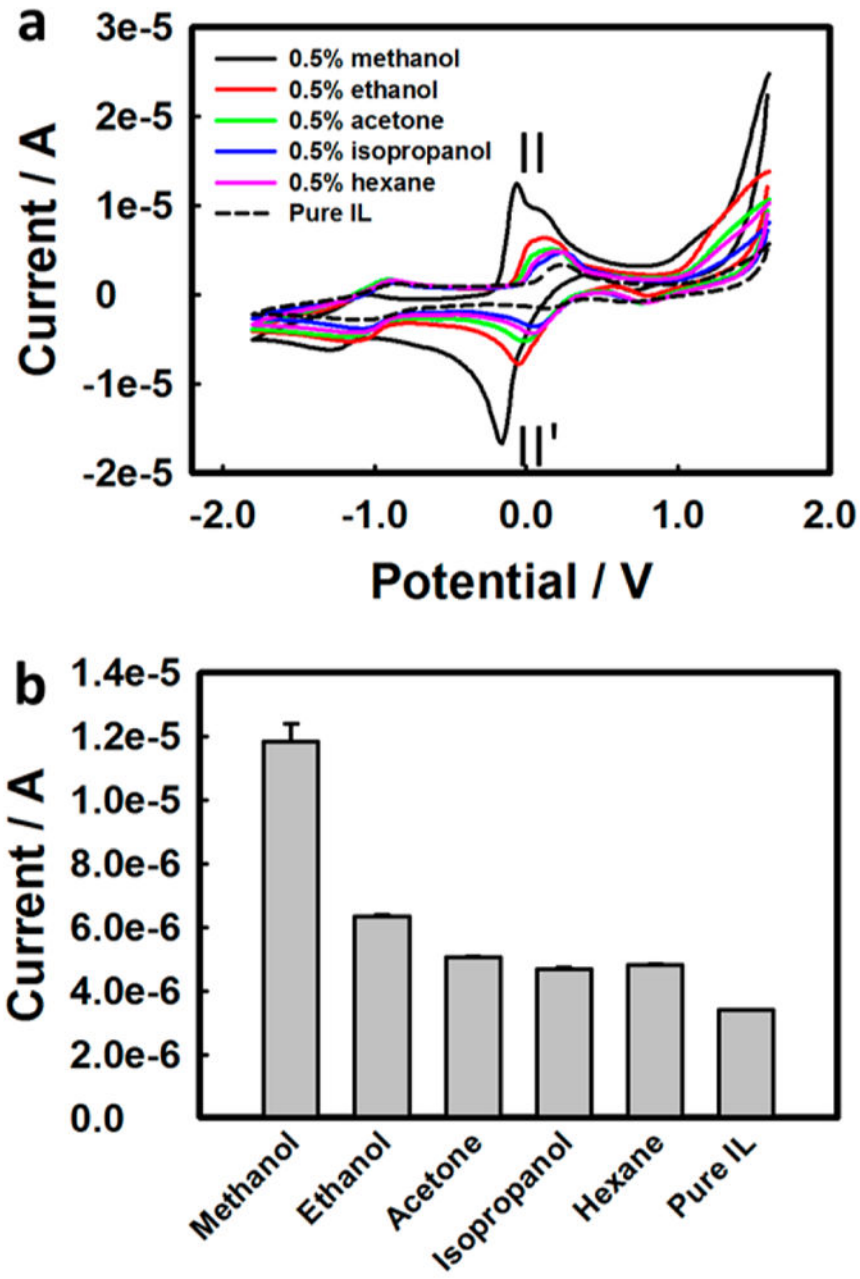

Figure 6.

(a) CVs for different analytes with 0.5% (v/v) concentration in [Bmpy][NTf_2] IL in nitrogen at Pt electrode. (b) Current plot obtained from peak II in (a).